Investigation of math xmlns="http://www.w3.org/1998/Math/MathML">mmultiscripts>mi>Ca/mi>mprescripts>/mprescripts>none>/none>mn>48/mn>/mmultiscripts>/math>-induced reactions with math xmlns="http://www.w3.org/1998/Math/MathML">mmultiscripts>mi>Pu/mi>mprescripts>/mprescripts>none>/none>mn>242/mn>/mmultiscripts>/math> and math xmlns="http://www.w3.org/1998/Math/MathML">mmultiscripts>mi mathvariant="normal">U/mi> mprescripts>/mprescripts>none>/none>mn>238/mn>/mmultiscripts>/math> targets at the JINR Superheavy Element Factory

Yu. Ts. Oganessian et al.

Phys. Rev. C **106**, 024612 — Published 22 August 2022

DOI: 10.1103/PhysRevC.106.024612

Investigation of ^{48}Ca-induced reactions with ^{242}Pu and ^{238}U targets at the JINR Superheavy Element Factory

Yu.Ts. Oganessian [1], V.K. Utyonkov [1], D. Ibadullayev [1,2], F.Sh. Abdullin [1], S.N. Dmitriev [1], M.G. Itkis [1], A.V. Karpov [1], N.D. Kovrizhnykh [1], D.A. Kuznetsov [1], O.V. Petrushkin [1], A.V. Podshibiakin [1], A.N. Polyakov [1], A.G. Popeko [1], R.N. Sagaidak [1], L. Schlattauer [1,3], V.D. Shubin [1], M.V. Shumeiko [1], D.I. Solovyev [1], Yu.S. Tsyganov [1], A.A. Voinov [1], V.G. Subbotin [1], A.Yu. Bodrov [1], A.V. Sabel'nikov [1], A. Lindner [1,3], K.P. Rykaczewski [4], T.T. King [4], J.B. Roberto [4], N.T. Brewer [4,*], R.K. Grzywacz [4,5], Z.G. Gan [6], Z.Y. Zhang [6], M.H. Huang [6], and H.B. Yang [1,6]

[1]*Joint Institute for Nuclear Research, RU-141980 Dubna, Russian Federation*
[2]*Institute of Nuclear Physics, 050032 Almaty, Kazakhstan*
[3]*Palacky University Olomouc, Department of Experimental Physics, Faculty of Science, 771 46 Olomouc, Czech Republic*
[4]*Oak Ridge National Laboratory, Oak Ridge, Tennessee 37831, USA*
[5]*Department of Physics and Astronomy, University of Tennessee, Knoxville, Tennessee 37996, USA*
[6]*Institute of Modern Physics, Chinese Academy of Sciences, Lanzhou 730000, China*

Experiments using a ^{48}Ca beam on ^{238}U and ^{242}Pu targets to produce superheavy nuclei were performed at the gas-filled separator DGFRS-2 on-line to the new cyclotron DC280 at the SHE Factory at JINR. The decay properties of ^{286}Fl and ^{287}Fl, as well as their α-decay products, were refined after the detection of 25 and 69 new decay chains, respectively. In addition, 16 decay chains of ^{283}Cn were observed in the ^{238}U+^{48}Careaction. The possibility of existing of isomeric states in the ^{287}Fl consecutive α decays is discussed. A new α line with an energy of 100-200 keV lower than the main one at 10.19 MeV was observed for the first time for even-even ^{286}Fl decay. A maximum cross section of $10.4^{+3.5}_{-2.1}$ pb was measured for the ^{242}Pu(^{48}Ca,3*n*)^{287}Fl reaction.

I. INTRODUCTION

We present the results of experiments with ^{238}U and ^{242}Pu targets performed at the Superheavy Element Factory (SHE Factory) of FLNR, JINR, Dubna. The new cyclotron DC280 accelerating heavy ions up to 10 $p\mu$A [1] is supplying beams at the SHE Factory. The reaction products are analyzed by means of the next implementation of Dubna Gas Filled Recoil Separator (DGFRS-2) [2]. This experiment as well as the previous study of the ^{243}Am+^{48}Ca reaction [3] were verifying and optimizing capabilities of the SHE Factory for the production and study of new isotopes of known superheavy elements up to Og (Z=118), as well as the synthesis of new elements with Z>118.

The ^{242}Pu+^{48}Ca reaction is planned to be used for further study of the chemical properties of element Fl (Z=114). A series of experiments were previously performed at FLNR with the insitu volatilization and on-line detection technique in combination with the cryo-online detector (COLD) [4] and at GSI with isothermal gas chromatography and thermochromatograph Cryo-Online Multidetector for Physics And Chemistry of Transactinides (COMPACT) [5]. The results of these experiments were found to differ. However, only few atoms of Fl were observed at each experiment.

Compared to the experiments on the synthesis and study of the decay properties of the heaviest nuclei performed at electromagnetic separators, the study of the chemical properties of superheavy elements has difficulties related to the longer transport time and correspondingly smaller efficiency.

To prepare and perform such experiments on the investigation of element Fl, it is necessary to establish more accurately the cross section at the maximum of the excitation function for the ^{242}Pu(^{48}Ca,3*n*) reaction, as well as the decay properties of ^{287}Fl ($T_{1/2}\approx$ 0.5 s) and its daughter nuclei.

[*]Current address: Premise Health, Brentwood, Tennessee 37027, USA

For applying physical preseparation of Fl ions before their entering the chemical apparatus, it is important to determine precisely the charge of the Fl ions in the filling gas of the separator and the horizontal and vertical distributions of recoils at the focal plane of DGFRS-2. It is also important to test the stability of the target at an increased beam intensity. The stability of the target at high beam intensities was also studied in a separate experiment with a ^{238}U target.

The reaction cross section and the decay properties of nuclei in the ^{287}Fl decay chain were first measured at DGFRS in 2003 [6-9]. This isotope was produced both in the direct reactions ^{242}Pu(^{48}Ca,3*n*) and ^{244}Pu(^{48}Ca,5*n*), and after decay of the parent nucleus ^{291}Lv, the product of the ^{245}Cm(^{48}Ca,2*n*) reaction. Descendants of ^{287}Fl were also observed in the ^{238}U(^{48}Ca,3*n*)^{283}Cn reaction [7]. In total, 19 decay chains of ^{287}Fl were registered in the reactions with ^{242,244}Pu and ^{245}Cm, as well as 7 decay chains of ^{283}Cn in the reaction with ^{238}U. The same isotopes were also observed in experiments on the study of the chemical properties of elements Cn [10] and Fl [4] (6 chains), as well as at the separators SHIP (1 chain of ^{291}Lv and 4 chains of ^{283}Cn [11-13]), BGS (1 chain of ^{287}Fl [14]), and GARIS-II (2 chains of ^{283}Cn [15]).

In the ^{242}Pu+^{48}Ca reaction, a lighter isotope ^{286}Fl [7] was also synthesized at DGFRS. This isotope was also observed as a daughter product of ^{294}Og [9,16,17] and ^{290}Lv [8,9]. The product of its α decay, ^{282}Cn, was observed in the reaction with ^{238}U [7]. Two decay chains of ^{286}Fl were also produced at the BGS separator in the ^{242}Pu+^{48}Ca reaction [14,18].

II. EXPERIMENT

Experiments with use of the ^{242}Pu and ^{238}U targets were performed during March-June, 2021, and September-October, 2021, respectively. Some parameters of experiments, as well as number of observed nuclei ^{286}Fl, ^{287}Fl, and ^{283}Cn and cross sections of their production in the ^{242}Pu+^{48}Ca and ^{238}U+^{48}Ca reactions are shown in Table I.

TABLE I. The ^{242}Pu and ^{238}U target thicknesses, laboratory-frame energies of ^{48}Ca in the middle of the target layer, resulting excitation energy intervals (with use of mass tables [19,20]), total beam doses, the numbers of observed decay chains assigned to ^{287}Fl (3*n*), ^{286}Fl (4*n*), and ^{283}Cn (3*n*) and the cross sections of their production.

Target thickness (mg/cm^2)	E_{lab}[a] (MeV)	E^* (MeV)	Beam dose $\times 10^{18}$	No. of chains 3*n* / 4*n*	σ_{3n} (pb)	σ_{4n} (pb)
^{242}Pu 10×0.76, 0.56, 0.35	242.5	37.1-40.7	11.2	65 / 11	$10.4^{+3.5}_{-2.1}$	$1.8^{+1.0}_{-0.6}$
	247.5	41.3-44.8	5.0	4 / 14	$1.2^{+1.2}_{-0.7}$	$4.8^{+2.1}_{-1.6}$
^{238}U 0.67	234.4	33.6-37.1	12.1	4 / 0	$0.5^{+0.5}_{-0.3}$	–
	231.1	30.7-34.4	13.5	12 / 0	$1.5^{+0.7}_{-0.5}$	–

[a] The beam energy was measured with a time-of-flight system, which has a systematic uncertainty of 1 MeV.

The targets consisted of the enriched isotopes ^{242}Pu (95.5%) and ^{238}U (99.3%) and were produced by electrodeposition on a 0.62-mg/cm^2 Ti backing. Targets consisted of 12 sectors which were mounted on a periphery of a disk with a diameter of 24 cm and 10-mm target layer opened for the beam and were rotated at 980 rpm. The total active surface area was 69 cm^2. The average thickness of the ^{238}U target was 0.67 mg/cm^2. Ten ^{242}Pu targets had an average Pu layer thickness of about 0.76 mg/cm^2, and two targets were 0.56 and 0.35 mg/cm^2 thick. This was done in order to check the dependence of the target stability on its thickness when irradiated with an intense ^{48}Ca beam. Throughout the experiment, the beam intensity was gradually increased. For about a week, a maximum beam intensity of 3 $p\mu$A was maintained on the ^{242}Pu target. The results of measurement showed, that stability of the targets did not depend on the thickness; no loss of substance was detected at the doses shown in Table I.

In the experiment with the ^{238}U target, the maximum beam intensity of ^{48}Ca was 6.5 *p*μA. When examining the target after two experiments (total beam dose of about 2.6×10^{19}), many small holes were found in it. However, the measurements of the α-particle activity of ^{238}U showed that about 97% of the substance was preserved on the Ti backing. The shape of the energy spectrum corresponded to that which was expected for a uniform layer thickness without the uneven thickening of matter or penetration of ^{238}U into the Ti backing. From the shift of the maximum of energy spectrum of α particles that passed through Ti backing (the target backing faced the detector), it can be concluded that its thickness increased slightly (e.g., due to accumulation of H_2 in Ti, deposition of oil from pumps on the surface of the Ti backing, etc, see also [21]), but the corresponding decrease of ^{48}Ca energy should not exceed 1-2 MeV.

The separator DGFRS-2 [2] was filled with hydrogen at a pressure of about 0.9 mbar, which was constantly pumped through the separator in the direction from the detector chamber to a differential pumping system installed in front of the target block. The detector chamber was separated from the DGFRS-2 volume by a 0.7-μm Mylar foil and filled with pentane at a pressure of 1.6 mbar.

The focal detector of 48 mm in vertical and 220 mm in horizontal directions consisted of two 48×128-mm double-sided silicon strip detectors (DSSD) (Micron Semiconductor Ltd.). They were mounted one by one in such a way that the front detector shielded part of the rear detector. Forty eight 1-mm front horizontal strips of both detectors were connected. The back strips were paired together to form 110 strips of 2 mm width. These detectors were surrounded by eight silicon single-sided 60×120-mm side detectors (SSSD), each with 8 strips, forming a box with a depth of 120 mm. All signals in detectors with amplitudes above the threshold (E_{th}) of 0.55–0.6 MeV were recorded independently by digital and analog data acquisition systems, similar to that employed at DGFRS [17]. The energy resolution when an α particle was registered with full energy (E_α) in the back or front strips, or by two neighboring horizontal or vertical strips of the DSSD, or simultaneously by the focal (E_f) and side (E_s) detectors is different. For α's registered solely by the side detector, the energy E_α was determined as $E_s+E_{th}/2$ and uncertainty as $E_{th}/2\times0.68$. In Appendixes A-C, we present energies which were recorded with the best resolutions. These values represent the standard deviations measured for ^{217}Th α line (E_α=9.26 MeV) in calibration experiments for different variants of registration of α particles.

Two multiwire proportional chambers (MWPC) were installed in front of the detectors for registration of nuclei passing through the separator [2]. Analog electronics was implemented for on-line registration of spatial, energy, and temporal correlations of evaporation residues (ER) and α particles, registered with full energy in the DSSD, with parameters expected for implantation of a nucleus in detectors and following α decay of Fl or daughter nuclei (namely, energies of events and ER-α time intervals). This pair of correlated events caused the beam to be switched off, in about 0.1 ms after registration of the first relevant α particle, to observe decays of descendant nuclei under low background condition.

III. RESULTS AND DISCUSSION

The energies of α particles or fission fragments and decay times of nuclei in the chains originating from ^{287}Fl and ^{286}Fl are given in Appendixes A and B, respectively.

The decay chains of ^{287}Fl terminated by spontaneous fission (SF) of ^{279}Ds in which two α particles (or one in the case of SF of ^{283}Cn) occurred but were lost due to incomplete registration efficiency by the detector should be observed as ER-SF sequences. However, in this case, the probability of observing correlations of random particles that do not originate from ^{287}Fl increases significantly. The total expected number of random ER-SF chains was estimated from experimental data based on the number of α-like events, number of their random correlations with recoils (recoil energies E_R>7 MeV, time intervals $\Delta t_{R-\alpha}$<10 s), and number of observed SF events. For the entire experiment, we could expect about one such correlation. In the experiment at the energy of 243 MeV, we registered three such chains, which we do not include in Appendix A and do not discuss

further. Obviously, the number of random correlations, such as those shown in Appendix A, should be several orders of magnitude lower due to the registration of one or more additional α particles in the chains.

On the contrary, decays of ^{286}Fl can be observed as ER-SF chains, since this isotope undergoes SF with a probability of about 40%, as was found in previous experiments [6]. The number of random correlations is expected to be less than 0.1, so we attribute all of the chains shown in Appendix B to ^{286}Fl.

The data measured in the decay chains originating from ^{283}Cn observed in the ^{238}U(^{48}Ca,3*n*) reaction are given in Appendix C. Two of the 16 chains were registered as ER-SF sequences. The number of random ER-SF sequences with E_R>10 MeV and $\Delta t_{R\text{-}SF}$<2 s is less than 0.006. We included these ER-SF events in Appendix C with ^{283}Cn chains, but their characteristics were used only when calculating the reaction cross section.

The energy spectra and lifetime distributions of α particles of ^{287}Fl, ^{283}Cn, ^{279}Ds, ^{275}Hs, ^{271}Sg, and ^{267}Rf (only lifetime distribution) observed in [4,6-15] and this work are shown in Fig. 1. For α-particle spectra, the events with an energy resolution better than 40 keV (the full width at half maximum (FWHM)<95 keV) were chosen. For distribution of decay times, only decays after the registered nearest precursor were selected.

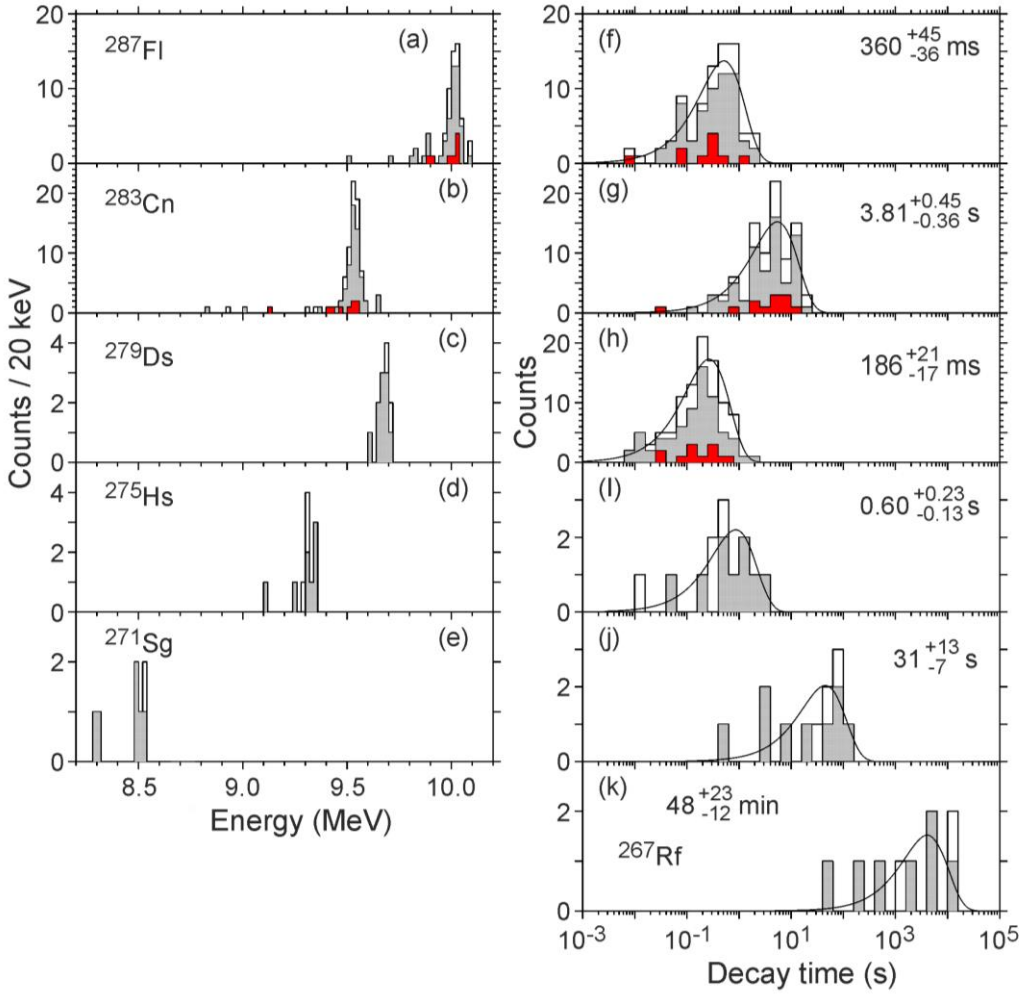

FIG. 1. Alpha-particle energy spectra (a) − (e) and decay-time distributions on a logarithmic scale (f) − (k) for ^{287}Fl, ^{283}Cn, and descendant nuclei. The data observed in this work and a summary of known results are shown by gray and open histograms, respectively. Alpha-particle energies and decay times of ^{287}Fl and ^{283}Cn followed by α decay of ^{279}Ds as well as lifetimes of α decays of ^{279}Ds are shown in red. The smooth curves are the time distributions for exponential decays calculated with the half-lives $T_{1/2}$ shown in the figures.

The number of newly registered decays of ^{287}Fl is three times larger than the number of nuclei synthesized in all previous experiments, which allows us to better determine their decay properties.

To identify the nuclei in cases when the intermediate links in the α-decay chains were lost or SF did not relate to the final nucleus ^{267}Rf, we used the difference in the α-decay energies and half-lives of the nuclei, which were established in previous experiments [4,6-15] and this work. The validity of this assignment is confirmed by the fact that the distributions of decay times for most of the observed isotopes from ^{286,287}Fl to ^{267}Rf satisfy the criterion for a single radioactive species suggested in [22]. Only for ^{271}Sg does the standard deviation of the logarithm of the measured decay times ($\sigma(\ln t)_{exp}$=1.78) exceed the 95-% confidence interval of 0.72-1.77 suggested in [22] for 13 events originating from a single exponential distribution. However, in the very first ^{287}Fl decay chain, in which the α decay of ^{279}Ds was registered [7], spontaneous fission with a time of 381 s was attributed to ^{271}Sg. This value is almost four times higher than the longest decay time of all of the other 12 events recorded later and attributed to ^{271}Sg. One cannot exclude that the fission in this chain was caused by ^{267}Rf, and α decay of ^{271}Sg was not registered. In this case, for the remaining 12 decays, the value $\sigma(\ln t)_{exp}$=1.66 fits into the interval 0.70-1.79 [22]. This long time of 381 s is not shown in Fig. 1 and was not included in calculation of the half-life of ^{271}Sg.

Due to significantly higher statistics, the properties of the nuclei have been determined with better accuracy. The half-lives measured in this work are 0.33±0.04 s, $3.7^{+0.5}_{-0.4}$ s, 0.18±0.02 s, $0.78^{+0.38}_{-0.19}$ s, 28^{+14}_{-7} s, and 40^{+23}_{-11} min for isotopes ^{287}Fl, ^{283}Cn, ^{279}Ds, ^{275}Hs, ^{271}Sg, and ^{267}Rf, respectively. Especially large difference with respect to the earlier data [6] are observed for ^{275}Hs, ^{271}Sg, and ^{267}Rf. Note that in former studies only four decay chains were observed in which ^{279}Ds underwent α decay. The energy spectra of the newly measured α particles are in a good agreement with the spectra presented in [6] for the mentioned isotopes. However, it should be noted that the half-life of ^{287}Fl was lower than the previously measured value (0.36±0.04 s instead of $0.48^{+0.14}_{-0.09}$ s), which might reduce the overall detection efficiency in the Fl chemistry studies.

In the α-particle spectra of odd-*N* nuclei, less intense lines are clearly visible along with the main peaks. Only the spectrum of α particles of ^{279}Ds looks like a single line. Possibly this is an effect of insufficient statistics caused by the large SF branch for this nucleus. However, the spectra of the daughter nuclei ^{275}Hs and ^{271}Sg consist of more than one line. If we select from the α particles of ^{287}Fl and ^{283}Cn only those followed by α decay of ^{279}Ds, one can see a slight difference between their energy spectra and the summary α-particle spectra of these isotopes. The distributions of α-particle energies and decay times of such events are shown by red histograms in Fig. 1. It seems that a relatively large part of the energies of such particles fall into the lower energy region of the spectrum. For example, 11 out of 66 events (17%) of the total spectrum of ^{287}Fl were registered with E_α<9.94 MeV, but a larger part, 2 out of 8 events (25%), which led to α decay of ^{279}Ds were observed in this low-energy region. For α particles of ^{283}Cn with E_α<9.44 MeV, these ratios are 9/82 (11%) and 3/9 (33%), respectively. One can note that the α-particle energy of ^{291}Lv in the chain that was followed by α decay of ^{279}Ds in [12,13] also turned out to be 0.24 MeV lower than those registered in the chains that led to the fission of ^{279}Ds [6]. Besides, the half-lives of such decays of ^{287}Fl and ^{283}Cn are slightly lower than those determined from the sum of events $T_{1/2}=0.21^{+0.10}_{-0.05}$ s and $2.8^{+1.1}_{-0.6}$ s, respectively (compare with the data in Fig. 1). The half-life of ^{279}Ds determined from its α decay is $0.16^{+0.06}_{-0.04}$ s, similar to the value calculated from all events. It is obvious that these observations are based on a low number of events and further research is required to confirm or refute them. If this is really the case, this feature could mean that the level structure of nuclei involved in α decay affects the probability of fission. A similar feature is present in ^{261}Rf, which has two states with $T_{1/2}$=68 s, E_α=8.28 MeV, SF branch b_{SF}<0.11 and $T_{1/2}$=3 s, E_α=8.51 MeV, b_{SF}=0.91 (see, e.g., [23] and references therein). Recently the hindered spontaneous fission half-life by a factor of about 120 was observed for the high-spin ground state of ^{247}Md compared to its low-spin isomeric state [24].

The SF branch in ^{283}Cn decay was considered in [6,11,13,15]. In experiments with ^{242}Pu, the decay chain terminated with the SF of ^{283}Cn should be registered as an ER (^{287}Fl)-α (^{287}Fl)-SF (^{283}Cn) chain. The same signature of the ^{287}Fl decay will occur in case the ^{283}Cn α particle will not be registered due to the limited registration efficiency. On the one hand, in the ratio of 1/15 in the decays of ^{287}Fl registered in the ^{242}Pu+^{48}Ca reaction and 3/7 in the decays of ^{283}Cn in the ^{238}U+^{48}Ca reaction [7], the fission observed at the end of the chains could really belong to ^{283}Cn (the part of observed SF events to the total number of chains (P_{SF}) ≈18%). But in the same set of results, 3 out of 15 α particles of ^{287}Fl were not registered (probability ≈20%). From these observations, one can postulate that b_{SF} for ^{283}Cn is small, less than about 7% [6]. Note that α decay of ^{283}Cn was registered in other 12 chains in [4,8-10,12,14], however, in all cases ^{283}Cn was produced as a descendant nucleus. On the other hand, in 3 of the 7 decays of ^{283}Cn observed in the direct reaction ^{238}U+^{48}Ca [7], fission could be caused by SF branch of ^{283}Cn, and in a half of the 6 chains produced in the same reaction in [11,15], SF was attributed to ^{283}Cn.

In the experiments with ^{242}Pu, in 10 of the 69 chains shown in Appendix A (P_{SF}≈14%), α decay of ^{283}Cn was not observed and the terminal SF could be assigned to ^{283}Cn. However, in six chains, α particles of ^{287}Fl were also not registered (i.e., the probability of losing α particle is ≈9%). From this observation we can estimate b_{SF} of about 6% for ^{283}Cn, without taking into account the efficiency of registration of α particles, which would reduce this value by about 5-10%.

In 16 chains from the experiment with a ^{238}U target, we observed two ER-SF sequences which can be caused by both spontaneous fission of ^{283}Cn and non-registration of its α particle. From these data, the upper limit of 21% for the SF branch of ^{283}Cn can be set with a confidence level of 84%.

Because of the remaining uncertainty, we did not include in Fig. 1 and in the estimates of half-life of ^{283}Cn those decays in which α decay of ^{283}Cn was not observed.

The structure of low-lying one-quasineutron states of nuclei in the decay chain of ^{287}Fl was predicted in [25]. Due to the hindrance for SF from states with a large K (projection of the angular momentum onto the symmetry axis of the nucleus), the fission of ^{279}Ds can occur with the higher probability from the low-K isomeric state (i.s.) $1/2^+[611]$ and α emission would de-excite the high-K ground state (g.s.) $5/2^+[613]$ (see Fig. 1 in [25]).

These calculations resulted in a good agreement between the experimental and theoretical Q_α values, e.g., α-decay energies of ^{287}Fl (10.06 MeV), ^{279}Ds (9.67 MeV), ^{275}Hs (9.25 MeV), and ^{271}Sg (8.51 MeV) coincide with the experimental data within about 200 keV, see Table II. In addition, a reduced energy (Q_α=9.77 MeV) was predicted for ^{283}Cn in the decay chains leading to α decay of ^{279}Ds, to be compared to that for chain leading to fission of ^{279}Ds (Q_α=10.11 MeV).

The decay properties of nuclei in the ^{287}Fl chain are given in Table II. When evaluating the decay branch, all known events were taken into account. The efficiencies of registration of α particles by the detectors were estimated from the numbers of missing particles in the corresponding experiments and/or facilities.

Table II. Summary decay properties of isotopes extracted from previous and present studies. The first three columns show nucleus, decay mode and branch, as well as half-life. The next four columns show α-particle energy E_α, α-decay energy Q_α, and partial half-lives with respect to α decay and SF.

Nucleus	Decay mode, branch (%) [a,b]	Half-life [b]	E_α (MeV) [c]	Q_α (MeV) [c]	T_α [b]	T_{SF} [b]
^{287}Fl	α: >70	360^{+45}_{-36} ms	10.016(15)	10.157(15)		>1 s
^{286}Fl	α: 55±8	105^{+17}_{-13} ms	10.191(10)	10.335(10)	$0.19^{+0.05}_{-0.04}$ s	$0.23^{+0.07}_{-0.04}$ s
^{283}Cn	α: 96^{+3}_{-6} [d]	$3.81^{+0.45}_{-0.36}$ s	9.531(15)	9.667(15)	$4.0^{+0.5}_{-0.4}$ s	90^{+160}_{-50} s
^{282}Cn	SF	$0.83^{+0.18}_{-0.13}$ ms				
^{279}Ds	SF: 87^{+2}_{-5}	186^{+21}_{-17} ms	9.686(15)	9.827(15)	1.4±0.4 s	$0.22^{+0.02}_{-0.03}$ s

^{275}Hs	α:>89	$0.60^{+0.23}_{-0.13}$ s	9.323(15)	9.461(15)	<0.9 s	>4 s
^{271}Sg	α: 73^{+10}_{-15}	31^{+13}_{-7} s	8.501(16)	8.629(16)	43^{+21}_{-11} s	120^{+90}_{-50} s
^{267}Rf	SF	48^{+23}_{-12} min				

[a] Branch is given for the most probable decay mode (α or SF). The branching ratio is not listed when only one decay mode was observed.

[b] Error bars correspond to 68%-confidence level.

[c] Energy uncertainties given in parenthesis correspond to the data with the best energy resolution.

[d] Branch is determined from the data where ^{283}Cn was observed as the daughter nucleus after α decay of ^{287}Fl, see the text.

In the ^{242}Pu+^{48}Ca reaction, along with 69 decay chains of ^{287}Fl, we also registered 25 decays of the neighboring isotope ^{286}Fl (Appendix B). Spontaneous fission of ^{286}Fl was registered in 11 of the 25 decay chains. Such a number of α decays and SF events is in a good agreement with the known branch for the α decay of this isotope, $b_\alpha=60^{+10}_{-11}$% [6]. The parameters of these chains differ clearly from those observed in the decays of spontaneously fissioning isomers in [7] as well as in this work. In addition to 11 ER-SF decay chains attributed by us to fission of ^{286}Fl, we registered 12 other recoil-SF chains with energy interval of recoils within 0.9-4.3 MeV which is noticeably lower than the implantation energies of ^{286,287}Fl (≥8.5 MeV). Their fragment energies (106-161 MeV) are also systematically lower than those of ^{286}Fl, and the lifetimes were 18.4 ms, 0.69 ms, 0.14 ms and less than 41 μs for the remaining 9 events. The later values are consistent with the half-lives of SF isomers of ^{242mf}Am, ^{240,244mf}Am, and several Pu and Am isomers with half-lives ranging within 1-73 μs [26], which can be produced in few-nucleon transfer reactions with ^{242}Pu.

As mentioned above, in previous experiments at DGFRS, the isotope ^{286}Fl was observed as an α-decay product of parent nuclei produced in the reactions ^{249}Cf(^{48}Ca,3*n*)^{294}Og (5 decay chains [9,16,17]) and ^{245}Cm(^{48}Ca,3*n*)^{290}Lv (12 chains [8,9]), as well as in the direct reaction ^{242}Pu(^{48}Ca,4*n*)^{286}Fl (9 chains [7]). Two more chains were observed in the later reaction studied at BGS [14,18].

Recently, two new decay chains were observed and assigned to ^{286}Fl in the experiment where the target wheel consisting of one segment of enriched ^{242}Pu and three segments of enriched ^{244}Pu was irradiated by ^{48}Ca [27]. In the first one, the parameters of the signals in the ER-α-SF chain correspond well to the decay chain originating from ^{286}Fl. In the second ER-α-SF sequence, the α-decay event consisted of signals of 9.60 MeV in the focal detector, which is approximately 0.6 MeV lower than the average energy value for ^{286}Fl, and 0.36 MeV in the upstream one. This pair was observed within a beam-off interval where counting rate of random events was 8 times lower than that in the beam-on period. Such a ratio of energies in the focal and side detectors is extremely rare for the case when one α particle leaves the focal detector and stops in the side one. Most of the energy of the α particle is usually released in the side detector. This signal in the side detector with *E*=0.36 MeV was interpreted as arising from a converted electromagnetic transition.

In the 14 decay chains of ^{286}Fl observed in [7-9,14,18], the lower limit of α-particle energy, after taking into account the uncertainties (68% confidence level), was larger than 9.9 MeV. In the 13 chains shown in Appendix B, only in one case the energy of 9.92±0.20 MeVcan be considered as not much different from the value of 9.6 MeV due to a large uncertainty, i.e., only one α-particle energy of ^{286}Fl out of 27 measured earlier. Thus, the energy of 9.60 MeV was not observed in the chains, the number of which exceeds the result [27] by an order of magnitude. This fact does not indicate obvious contradictions between different measurements, but points to a need for further studies of ^{286}Fl and ^{282}Cn decay properties.

The energy spectrum of ^{286}Fl and lifetime distributions of ^{286}Fl and ^{282}Cn observed in [7-9,14,16-18,27] and this work are shown in Fig. 2.

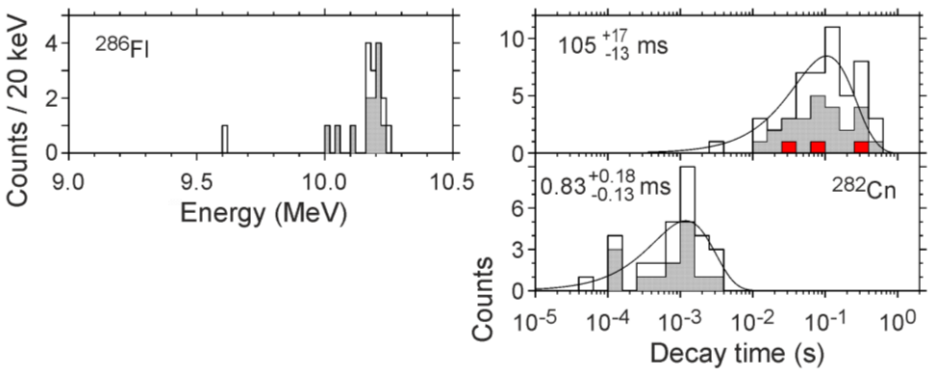

FIG. 2. The same as in Fig. 1 but for ^{286}Fl. Decay times of the three low-E_α events of ^{286}Fl are shown in red.

The new data are in a good agreement with the previously known results. The half-lives measured in this work are 91^{+22}_{-15} ms and $0.71^{+0.25}_{-0.15}$ ms for ^{286}Fl and^{282}Cn, respectively. The energy spectrum of the newly measured α particles is also in agreement with the spectrum presented in [6] for ^{286}Fl. The decay properties of ^{286}Fl and ^{282}Cn, estimated with the use of all known data, are given in Table II.

For the even-even ^{286}Fl we detected for the first time three α particles with E_α=10.003±0.036, 10.050±0.027, and 10.109±0.016 MeV which differ, taking into account energy uncertainties, from the energy of the main line at 10.19 MeV. Their decay times are highlighted in red in Fig. 2. The last of the three energy values is slightly different from the first two values when using error bars corresponding to a 68% confidence level (c.l.). However, it seems unlikely that two additional lines of the main $0^+ \rightarrow 0^+$ α transition may be observed with comparable yield in an even-even nucleus. Moreover, the values of all energies do not contradict each other when using uncertainties corresponding to c.l. of 95%, and even more, to the full width at half maximum. Taking this into account, one can estimate the energy of an additional peak as E_α=10.054±0.053 MeV which is lower than that of the main line by about 100-200 keV.

A possible origin of such α transitions is decay to the first rotational 2^+ state of ^{282}Cn. Based on the two-center shell model [28,29] one can obtain β_2 = 0.18, β_4 = -0.08 for the g.s. deformation of ^{282}Cn. Similar values β_2 = 0.15, β_4 = -0.06 were obtained in the recent work [30]. The corresponding energy of the first 2^+ rotational state can be estimated as $\left(E_{2+} = \frac{\hbar^2 l(l+1)}{2\mathcal{J}_\perp}\right)_{l=2}$. This will lead to E_{2+} = 75 keV with the cranking model [31] used to calculate the moment of inertia $\mathcal{J}_\perp$. The corresponding decay branch for the α decay to the ground state (0^+) and the first rotational 2^+ state are estimated following [32] as 67% and 33%, respectively. The corresponding experimental values are about 82% and 18%. The observed difference between calculated and measured values of the decay branching ratio can be associated with two factors: low statistics for the decay to the excited state and/or overestimated values of β_2 deformation. The underestimated value of the energy of 2^+ state additionally supports the latter explanation. Following this analysis, one may try to estimate the value of the g.s. deformation of ^{282}Cn based on the measured branching ratio. The same approach described above will result in β_2 = 0.13 and E_{2+} = 101 keV for the 82% vs. 18% branching ratio for 0^+ and 2^+ states. The energy of the 2^+ state is thus in agreement with the experimentally observed 100-200 keV interval. Note, the energy spread of the three α particles may be due to the registration of a partial summing of their energies with conversion electrons, which may have occurred at de-excitation of daughter level 2^+.

Another explanation is based on predicted isomeric states. A scheme of two-quasiparticle states for ^{286}Fl and descendants was suggested in [25]. According to calculations, the energy of 10.05 MeV may be caused by population in the direct ^{242}Pu+^{48}Ca reaction of a two-quasiproton isomeric state 5^+_π in ^{286}Fl and subsequent decay to the same level 5^+_π in ^{282}Cn. The γ de-excitation of ^{282}Cn

from i.s. to g.s. is followed by fission. The α-decay energies Q_α from the g.s.-to-g.s. and from the i.s.-to-i.s. were predicted to be 10.38 and 10.16 MeV, respectively [25]. Thus, both the g.s. and, with a lower probability, i.s. may be populated in a direct reaction. There is good agreement between the experimental and theoretical results for both α-decay energy for the g.s.-to-g.s. transition $^{286}\mathrm{Fl}\xrightarrow{\alpha}{}^{282}\mathrm{Cn}$, and for the difference in Q_α for transitions through the g.s. and i.s. of ^{286}Fl and ^{282}Cn. This would mean the first observation of an α decay through i.s. in even-even superheavy nuclei produced in the ^{48}Ca-induced reactions.

It should be noted that the possible existence of 50-keV less energetic line in α decay of ^{288}Fl was discussed in [33]. As a result of the observation of 11 new decays of ^{288}Fl in [27], the average α-particle energy of this isotope was fixed at 9.92±0.01 MeV. The existence of an additional line was strictly rejected.

Summarizing, we conclude that gathering large statistics in experiments for synthesis of superheavy nuclei opens a door to spectroscopy of those nuclei and thus to more detailed experimental information on their ground- and isomeric-state properties. Clarification of the nature of these observed decays with lower energy α particles will require an increase of statistics as well as measuring α particles in coincidence with photons and/or conversion electrons.

In experiment with ^{242}Pu, the projectile energies were chosen to be close to the expected maximum of the 3*n*- and 4*n*-evaporation channels. For the 4*n* channel, the measured cross sections do not contradict the values measured in [7,18], see Fig. 3. The maximum cross section of the 3*n*–evaporation channel exceeds the value measured in [7] by a factor of about 3. The cross section for the $^{243}\mathrm{Am}(^{48}\mathrm{Ca},3n)^{288}\mathrm{Mc}$ reaction, measured at DGFRS-2 in recent experiments [3], also turned out to be higher than the values published in [34]. In part, such differences may be attributed to the low number of nuclei registered in previous experiments. In addition, the increased cross-section value may be explained by the fact that the projectile energy in current experiments was closer to the maximum of the excitation function than in [7]. Based on the dotted lines in Fig. 3, one could estimate an excitation-function width at half maximum of about 5-6 MeV. A change in the energy towards the maximum of the excitation function can result in a noticeable increase of the cross-section value. Also, the setting of magnetic elements of DGFRS, affecting the transmission, as well as an accuracy of estimation of the target thickness and the beam dose, influence the estimated value of the cross section. According to [35,36], a transmission of 50% was used for calculation of the cross sections for targets with a thickness of 0.76 mg/cm^2.

The same transmission value was used for calculations of the cross sections of the reaction of 0.67-mg/cm^2 ^{238}U with ^{48}Ca (Fig. 3). The cross section at the excitation energy of the compound nucleus ^{286}Cn of about 35 MeV turned out to be slightly lower than the values measured earlier in our experiments [7] and at GARIS-II [15]. However, it can be noted that only four chains out of seven in [7] and half of the chains observed at SHIP [11] and GARIS-II [15] were registered as ER-α-SF chains. In the remaining events, the ER-SF sequences were observed. Taking into account the low fission branch for ^{283}Cn, which was determined from the increased number of events, it cannot be excluded that in these experiments mainly ER-α-SF chains belong to the decay of ^{283}Cn. In this case, the cross sections of the reaction measured earlier in [7,11,15] may be up to two times lower.

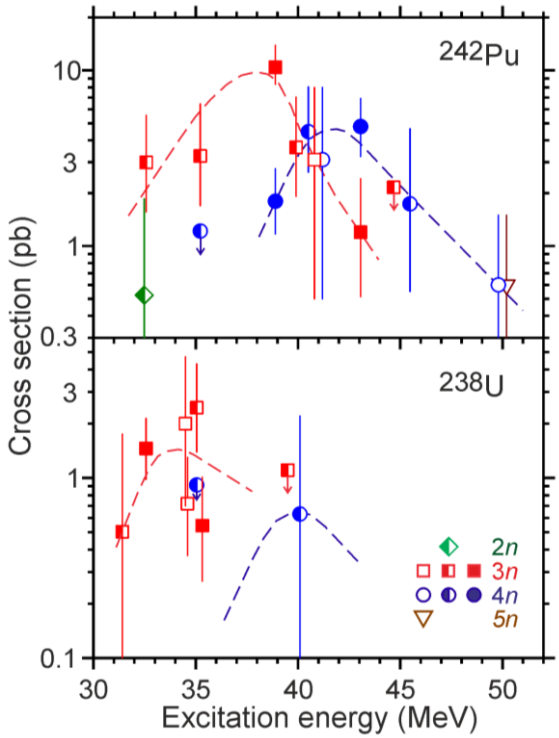

FIG. 3. Cross sections for the 2*n*- to 5*n*-evaporation channels for the ^{242}Pu+^{48}Ca and ^{238}U+^{48}Ca reactions. Vertical error bars correspond to total uncertainties. Symbols with arrows show upper cross-section limits. Data shown by open, half-closed, and closed symbols are from [11,15,18], [7], and this work, respectively. The dashed lines through the data are drawn to guide the eye.

IV. SUMMARY

The ^{242}Pu+^{48}Ca reaction has been studied at two projectile energies at the new separator DGFRS-2 demonstrating an enhanced discovery potential for further studies of physical and chemical properties of superheavy elements. The decay properties of ^{286}Fl and ^{287}Fl, as well as their descendants, have been refined from 25 and 69 new decay chains, respectively.

The maximum cross section of the 3*n*-evaporation channel leading to ^{287}Fl was measured to be about three times larger than in previous studies.

In the experiment with the ^{238}U target, the maximum beam intensity of ^{48}Ca was 6.5 *p*μA and a total beam dose of 2.6×10^{19} was collected. Many small holes were found in the target sectors but the measurements of the α activity of ^{238}U showed that about 97% of the substance was preserved on the Ti backing. 16 new decay chains of ^{283}Cn were observed at two projectile energies.

Two different α transitions in the decay chains starting with ^{287}Fl and leading to α decay of ^{279}Ds in one case and its SF in another one may follow from somewhat different α-particle energies and half-lives of ^{287}Fl and ^{283}Cn, indicating the decays connecting low-energy excited states and ground states.

A new α line with energy of 100-200 keV lower than the main peak was observed for the first time for even-even ^{286}Fl. A possible origin of this line, namely a population of the rotational 2^+ state of ^{282}Cn or a transition connecting isomeric states in ^{286}Fl and ^{282}Cn is discussed.

ACKNOWLEDGMENTS

We thank the personnel operating the DC280 cyclotron and the associates of the ion-source group for obtaining ^{48}Ca beams. These studies were supported by the Ministry of Science and Higher Education of the Russian Federation through Grant No. 075-10-2020-117 and by the JINR Directorate grant. Research at ORNL was supported by the U.S. DOE Office of Nuclear Physics

under DOE Contract No. DE-AC05-00OR22725 with UT Battelle, LLC. This work was also supported by the Strategic Priority Research Program of Chinese Academy of Sciences (Grant No. XDB34010000).

APPENDIX A

Observed decay chains originating from ^{287}Fl. The first three columns show lab-frame beam energy in the middle of the target layer and dipole D1 rigidity, decay-chain number and date of registration, ER energy and position on detector. For the following decays the α-particle and spontaneous fission fragment energies and the time intervals between events are shown. Bold events were registered during a beam-off period. The α-particle energy errors are shown in parentheses. If the total energy of α particles was not recorded (the particle escaped DSSD, leaving low energy in it, and did not enter SSSD, or leaved DSSD with deposited energy below the threshold value and stopped in SSSD, or one of the strips was not registered, we give the probability that the particle originates from a random event and does not belong to a chain of successive decays. If the particle was observed, but this probability was calculated to be larger than 10%, or the particle was not observed at all, "missing α" is indicated in the corresponding cell. Time intervals for α particles following a "missing α" were measured from preceding registered events and are shown in italics.

E_{lab} Bρ (Tm)	No Date d/m	E_{ER} (MeV) (y,x) (mm)	^{287}Fl E_α (MeV) t_α (ms) P_{ran}	^{283}Cn E_α (MeV) t_α (s) P_{ran}	^{279}Ds $E_{\alpha/SF}$ (MeV) $t_{\alpha/SF}$ (s) P_{ran}	^{275}Hs $E_{\alpha/SF}$ (MeV) $t_{\alpha/SF}$ (s) P_{ran}	^{271}Sg $E_{\alpha/SF}$ (MeV) $t_{\alpha/SF}$ (s) P_{ran}	^{267}Rf E_{SF} (MeV) t_{SF} (h)
242.5	1	14.85	2.814 [a]	9.500(31) [b]	205.8 [b]			
2.449	19/03	12,99	93.8	0.6536	0.1489			
			0.0001					
	2	15.20	10.037(16)	**Missing α**	**182.6** [b,c]			
	20/03	33,115	596.7		***2.9926***			
	3	12.91	10.033(21)	**9.551(21)**	**213.3**			
	20/03	33,47	772.1	**11.098**	**0.5076**			
	4	11.91	9.893(17)	**9.577(29)** [b]	**143.4**			
	20/03	35,103	400.1	**4.6640**	**0.2362**			
	5 [d]	13.77	10.049(22)	9.527(22)	201.1			
	22/03	36,-	299.2	2.3433	0.1837			
			0.0001	0.0006	0.0003			
	6	16.29	3.398 [a]	9.565(30) [b]	200.6 [b]			
	22/03	41,93	513.7	1.5378	0.0125			
			0.05					
	7	12.37	10.006(17)	**9.573(32)** [b]	**206.5**			
	23/03	23,175	35.04	**12.036**	**0.04274**			
	8	18.83 [e]	10.024(24) [e]	**9.573(33)** [b,d]	**223.7** [e]			
	24/03	4,114	198.6	**2.2882**	**0.3614**			
				0.0001				
	9	11.80	10.019(16)	**9.529(16)**	**193.7**			
	27/03	14,155	60.04	**2.3654**	**0.1274**			
	10	13.40	Missing α	9.551(16)	**183.3** [b]			
	27/03	22,125		*12.9521*	**0.0489**			
	11 [e]	12.50	10.050(23)	1.120 [a]	200.6 [b]			
	26/04	18,64	973.4	4.8312	0.1926			
				0.02				
	12	11.45	10.046(16)	**9.486(16)**	**174.6** [b]			
	27/04	23,37	80.93	**4.5542**	**0.7098**			
	13 [e]	15.59	10.012(23)	1.835 [a,f]	Missing α	9.352(23)	184.1 [b]	
	27/04	10,196	301.6	3.1146		*0.0329*	20.6939	
				0.01				
	14	12.34	5.339 [a]	9.542(19)	**9.712(19)**	**143.9** [g]		
	27/04	30,9	584.2	4.4897	**0.1505**	**1.4927**		

			0.001					
	15	12.08 [e]	10.048(23) [e]	9.567(23)	193.9			
	27/04	16,176	913.6	7.5340	0.8894			
	16	10.90	9.878(30) [b]	9.526(17)	175.1 [b]			
	27/04	21,161	768.4	7.4672	0.1010			
	17	11.73 [h]	9.808(30) [b]	Missing α	226.9 [c]			
	28/04	41,137	260.9		*1.8629*			
	18	10.92	Missing α	8.827(26) [b]	171.3			
	28/04	35,111		*13.5842*	0.0353			
	19	13.17	Missing α	9.530(16)	**9.690(16)**	**9.346(16)**	8.487(16)	181.2 [b]
	28/04	14,187		*4.5695*	**0.1927**	**0.1613**	104.76	1.3042
	20	11.80	9.910(33) [b]	9.404(17)	9.677(38) [b]	9.329(17)	8.489(17)	193.0 [b]
	28/04	24,175	333.6	6.2743	0.2589	0.9502	3.5595	0.5370
	21	14.97	10.027(16)	**9.129(30) [b]**	**9.656(32) [b]**	**9.109(16)**	8.503(29) [b]	182.0
	29/04	34,113	83.91	**2.1906**	**0.0387**	**0.4450**	92.856	1.6881
	22	10.83	9.509(16) [h]	9.32(20) [i]	203.4 [b]			
	30/04	24,35	285.1	0.1146	0.4097			
				0.01				
	23	11.74	10.035(16)	**9.544(33) [b]**	**200.4**			
	30/04	18,113	743.4	**11.3434**	**0.3716**			
	24	11.80	9.984(33) [b]	Missing α	225.4 [b,c]			
	15/05	47,105	101.0		*2.5047*			
	25	15.02	10.014(16)	**0.898 [a]**	**199.8**			
	19/05	29,209	308.0	**10.7681**	**0.0576**			
				0.001				
	26	12.37	9.888(33) [b]	Missing α	174.7 [b,c]			
	19/05	2,157	74.60		*0.0586*			
	27	11.10[e]	9.91(20) [i]	9.513(24)	**202.3[b]**			
	20/05	5,136	110.9	3.1898	**0.0114**			
			0.002					
	28	13.94	10.004(24)	**9.547(24)**	**132.5**			
	20/05	11,67	261.2	**2.1318**	**0.2265**			
	29	14.91	10.035(29) [b]	9.492(33) [b]	206.0			
	20/05	39,161	454.6	0.5383	0.0065			
	30	15.18	9.944(30) [b]	9.539(17)	**211.0 [b]**			
	21/05	20,161	1544.7	4.1415	**0.0236**			
	31	15.69	10.034(29) [b]	9.544(15)	**181.6 [b]**			
	22/05	34,173	443.8	4.2755	**0.1491**			
	32	13.66	9.887(16)	**9.522(32) [b]**	**9.668(16)**	**9.356(33) [b]**	**140.4**	
	23/05	29,177	1141.1	**0.9594**	**0.0308**	**3.1466**	**82.273**	
	33	12.83	Missing α	9.524(16)	**192.4**			
	24/05	35,155		*1.1165*	**0.2460**			
	34	12.47	9.713(31) [b]	9.523(33) [b]	196.8			
	24/05	11,177	659.7	3.0814	0.0154			
	35	11.88	9.90(20) [i]	9.549(16)	**209.1**			
	25/05	35,199	183.9	12.3620	**0.3780**			
			0.01					
242.5	36	11.19	9.985(33) [b]	9.556(16)	184.1			
2.421	26/05	16,211	73.63	4.3503	0.3667			
	37	10.89	9.836(16)	**9.523(16)**	**176.1 [b]**			
	26/05	36,137	6.949	**1.1942**	**0.2484**			
	38	12.04	9.886(42) [b]	9.371(22)	**178.9**			
	26/05	26,69	47.87	6.3045	**0.2917**			
	39	9.14	10.000(22)	**9.461(22)**	**191.3**			
	27/05	22,59	397.3	**2.8548**	**0.0810**			
	40	14.26	9.967(16)	**9.507(16)**	**201.0 [b]**			

	27/05	33,165	75.35	**15.7536**	**1.3193**				
	41	11.15	9.90(20) [i]	2.544[a]	9.696(19)	**Missing α**	**8.527(19)**	**208.9 [b]**	
	27/05	35,13	77.38	1.9091	0.1174		***54.4590***	**0.01496**	
			0.003	0.01					
	42	15.68	10.003(16)	**9.508(16)**	**193.1**				
	28/05	8,155	294.9	**13.7767**	**0.0709**				
	43	11.69	9.75(21) [i]	9.502(38) [b]	190.9 [b]				
	28/05	9,189	586.3	2.9311	0.1634				
			0.02						
	44	11.48	9.887(36) [b]	Missing α	163.6 [c]				
	28/05	13,27	1230.8		*2.5575*				
			0.0002						
	45	12.65	10.026(15)	**9.554(15)**	**181.8 [b]**				
	28/05	20,193	744.2	**4.0872**	**0.5135**				
	46	13.87	9.837(21)	9.29(20) [i]	181.3 [b]				
	29/05	37,45	202.6	1.6581	0.0985				
				0.10					
	47	12.74	10.019(32) [b]	9.019(33) [b]	183.9 [b]				
	29/05	40,101	967.8	0.9412	0.3306				
	48	14.12	10.031(30) [b]	9.649(32) [b]	176.3				
	29/05	23,113	69.60	4.7362	0.7043				
	49	12.82	10.010(16)	**9.520(16)**	**146.2 [b]**				
	29/05	22,131	758.9	**7.2802**	**0.0621**				
	50	13.00	10.005(17)	**9.522(17) [h]**	**223.7**				
	29/05	19,113	2454.7	**1.9155**	**0.2882**				
	51	12.52	10.000(32) [b]	Missing α	202.9 [b,c]				
	29/05	30,135	178.2		*2.9841*				
	52	14.72	10.087(28) [b]	9.652(22)	**200.9 [b]**				
	29/05	26,145	539.0	3.5748	**0.0084**				
	53	10.67	9.991(21)	**9.465(21)**	**9.699(21)**	**1.228 [a]**	**8.299(21)**	198.0 [b]	
	29/05	33,7	294.9	**6.0717**	**0.4043**	**0.0516**	**0.4777**	0.0641	
						0.0003			
	54	9.93	10.017(16)	**Missing α**	**136.8 [c]**				
	29/05	8,131	220.2		***4.9479***				
	55	14.12	9.979(27) [b]	Missing α	192.1 [c]				
	30/05	35,155	166.7		*3.9452*				
	56	10.58	9.998(23) [e]	**Missing α**	**146.8 [c,e]**				
	30/05	10,101	41.16		***3.2263***				
	57	13.05	10.055(27) [b]	9.544(21)	214.6 [b]				
	30/05	37,61	434.2	8.5983	0.2864				
	58 [h]	11.78	10.032(16)	9.510(16)	190.0 [b]				
	30/05	17,123	1639.0	0.8982	0.2368				
	59	11.82	Missing α	9.528(16)	**190.4**				
	30/05	11,179		*4.3424*	**0.2005**				
	60	10.93	9.996(17)	**9.528(17)**	**192.3**				
	30/05	21,25	449.8	**0.3204**	**0.0141**				
	61	12.84	10.020(23)	**9.494(31) [b]**	**168.2 [b]**				
	30/05	16,79	766.6	**1.7189**	**0.1758**				
	62	13.66	10.025(17)	**9.544(17)**	**185.9 [b]**				
	31/05	18,21	579.7	**3.4140**	**0.3230**				
	63	10.57	10.028(33) [b]	Missing α	9.679(33) [b]	9.244(16)	Missing α	190.4	
	31/05	15,99	159.5		*3.6985*	1.8515		2.9015	
	64	10.81	10.004(16)	**9.534(16)**	**182.4**				
	31/05	17,95	955.8	**4.4883**	**0.1694**				
	65 [e]	13.89	9.978(24)	**9.560(33) [b]**	**159.1**				
	31/05	46,180	31.42	**0.3085**	**0.1300**				
247.5	66	12.57	9.80(20) [i]	4.174 [a]	191.1 [b]				

2.421	02/06	14,161	929.7	0.5039	0.1837
			0.03	0.005	
	67	14.07	Missing α	9.648(16)	**202.0** [b]
	05/06	26,125		*1.2834*	**0.4852**
	68	14.16	9.999(21)	**Missing α**	**181.2** [b,c]
	06/06	33,81	139.2		***3.9158***
	69	14.14	1.501 [a]	9.558(22)	**173.1** [b]
	06/06	24,63	582.0	1.8092	**1.5108**
			0.004		

[a] Escaping α particle with only partial energy registered in focal detector.
[b] Event registered by both focal and side detectors.
[c] Tentative assignment– event might originate from SF of ^{283}Cn.
[d] X position was not registered.
[e] Event registered by two neighboring vertical strips.
[f] Tentative assignment–αparticles might originate from ^{279}Ds.
[g] Tentative assignment–SF event might originate from ^{271}Sg.
[h] Event registered by two neighboring horizontal strips.
[i] Escaping α particle registered by side detector only.

APPENDIX B

The same as Appendix A but for ^{286}Fl decay chains.

E_{lab} Bρ (Tm)	No Date d/m	E_{ER} (MeV) (y,x) (mm)	^{286}Fl $E_{\alpha/SF}$ (MeV) t_α (ms) P_{ran}	^{282}Cn E_{SF} (MeV) t_α (ms) P_{ran}
242.5	1	11.59	212.4 [b]	
2.449	27/03	20,17	262.9	
	2	12.06	10.202(33) [b]	205.7 [b]
	25/04	36,171	149.4	1.222
	3	15.88	9.92(20) [i]	202.7 [b]
	28/04	29,201	480.5	1.178
			0.004	
	4	9.16	10.003(36) [b]	184.2
	16/05	20,129	318.8	0.105
	5	10.23	178.4 [b]	
	20/05	41,93	106.2	
	6	13.33	10.173(17)	**147.0**
	21/05	5,145	22.84	**0.275**
	7	11.42	159.9	
	21/05	37,201	36.98	
242.5	8 [e]	12.62	10.050(27)	**186.7**
2.421	26/05	43,106	30.05	**0.149**
	9	12.70	10.214(15)	204.0 [b]
	27/05	23,143	196.9	0.419
	10	11.20	10.172(16)	**189.8** [b]
	31/05	40,47	280.2	**2.086**
	11	11.49	10.198(28) [b]	182.7 [b]
	01/06	21,115	285.8	2.788
247.5	12	13.26	10.213(22)	**196.9**
2.421	02/06	24,81	59.92	**0.865**
	13	8.48	10.187(29) [b]	113.0
	02/06	26,143	40.32	1.566
	14	13.39	10.220(17)	**175.7** [b]
	03/06	22,195	74.08	**1.365**
	15	14.02	10.109(16)	**202.4**

	03/06	11,119	64.53	**1.252**
	16 [e]	14.27	194.4 [b]	
	03/06	43,130	67.45	
	17	12.84	3.417 [a]	199.6
	03/06	24,123	30.02	0.883
			0.0002	
	18	11.91	174.0 [e]	
	04/06	14,72	76.17	
	19	10.73	192.8 [b]	
	04/06	38,171	236.7	
	20	13.31	192.2	
	05/06	28,153	80.92	
	21	14.85	197.8 [b]	
	05/06	21,189	53.23	
	22	9.46	140.2	
	05/06	27,81	144.6	
	23	14.43	192.5 [b]	
	05/06	29,187	10.90	
	24 [e]	12.61	213.8	
	06/06	15,58	142.3	
	25	12.04	10.209(32) [b]	146.1
	06/06	3,205	20.59	0.133

APPENDIX C

The same as Appendix A but for ^{283}Cn decay chains.

E_{lab} Bρ (Tm)	No Date d/m	E_{ER} (MeV) (y,x) (mm)	^{283}Cn E_α (MeV) t_α (s) P_{ran}	^{279}Ds $E_{\alpha/SF}$ (MeV) t_α (s) P_{ran}	^{275}Hs $E_{\alpha/SF}$ (MeV) t_α (s) P_{ran}	^{271}Sg $E_{\alpha/SF}$ (MeV) t_α (s) P_{ran}	^{267}Rf E_{SF} (MeV) t_{SF} (h)
234.4	1	11.39	9.530(22)	**117.0**			
2.415	01/10	24,79	12.5139	**0.7098**			
	2 [e]	11.33	9.598(30)	**129.2**			
	03/10	33,42	2.4971	**0.1991**			
	3	13.42	9.589(16) [h]	199.0 [b]			
	04/10	36,27	4.4295	0.0309			
234.4	4	12.22	9.511(18)	**188.6 [b]**			
2.454	04/10	39,51	13.1337	**0.2082**			
231.1	5	13.08	9.537(21)	**184.1 [b]**			
2.454	16/10	20,151	4.2992	**2.2575**			
	6 [e]	12.04	9.530(30) [b]	185.7 [b]			
	16/10	23,142	0.9672	0.3841			
	7	12.11	1.752 [a]	154.4			
	16/10	34,157	0.2845	0.0152			
			0.001				
	8 [e]	11.27	9.486(33) [b]	191.6			
	17/10	21,52	15.0573	0.0897			
	9	12.12	9.505(16)	**9.652(16)**	**9.305(16)**	**8.314(16)**	192.9 [b]
	17/10	45,27	6.6159	**0.1417**	**1.5355**	**2.7278**	0.1552
	10	12.30	9.550(29) [b]	202.7 [e]			
	22/10	21,71	4.2519	0.2475			
	11 [e]	10.12	9.557(30)	138.2			
	23/10	40,42	18.7076	0.0202			
	12	12.77	9.455(21)	**191.2 [e]**			
	23/10	47,153	13.4416	**0.0754**			

13	14.17	Missing α	171.3 [b,c]		
25/10	17,23		*1.6869*		
14	13.63	9.432(29) [b]	9.610(16)	**9319(16)**	**197.0**
26/10	23,13	11.4518	0.0932	**0.5036**	**7.8450**
15	10.81	Missing α	189.6 [c]		
26/10	22,123		*0.4196*		
16	12.77	9.531(17)	**158.8 [b]**		
26/10	24,29	10.6401	**0.1267**		

1. G. G. Gulbekian *et al*., Phys. Part. Nucl. Lett. **16**, 866 (2019).
2. Yu. Ts. Oganessian *et al*., Nucl. Instrum. Methods Phys. Res. A **1033**, 166640 (2022).
3. Yu. Ts. Oganessian *et al*. (unpublished).
4. R. Eichler *et al*., Radiochim. Acta **98**, 133 (2010).
5. A.Yakushev *et al*., Inorg. Chem. **53**, 1624(2014).
6. Yu. Ts. Oganessian and V. K. Utyonkov, Nucl. Phys. A **944**, 62 (2015); Rep. Prog. Phys. **78**, 036301 (2015).
7. Yu. Ts. Oganessian *et al*., Phys. Rev. C **70**, 064609 (2004).
8.Yu. Ts. Oganessian *et al*., Phys. Rev. C **69**, 054607 (2004).
9. Yu. Ts. Oganessian *et al*., Phys. Rev. C **74**, 044602 (2006).
10. R. Eichler *et al*., Angew. Chem. Int. Ed. **47**, 3262 (2008).
11. S. Hofmann *et al*., Eur. Phys. J. A **32**, 251 (2007).
12. S. Hofmann *et al*., Eur. Phys. J. A **52**, 180 (2016).
13. S. Hofmann *et al*., Eur. Phys. J. A **48**, 62 (2012).
14. L. Stavsetra, K. E. Gregorich, J. Dvorak, P. A. Ellison, I. Dragojević, M. A. Garcia, and H. Nitsche, Phys. Rev. Lett. **103**, 132502 (2009).
15. Daiya Kaji, Kouji Morimoto, Hiromitsu Haba, Yasuo Wakabayashi, Mirei Takeyama, Sayaka Yamaki, Yukiko Komori, Shinya Yanou, Shin-ichi Goto, and Kosuke Morita, Journal of the Physical Society of Japan **86**, 085001 (2017).
16. Yu.Ts. Oganessian *et al*., Phys. Rev. Lett. **109**, 162501 (2012).
17. N.T. Brewer *et al*., Phys. Rev. C **98**, 024317 (2018).
18. P. A. Ellison *et al*., Phys. Rev. Lett. **105**, 182701 (2010).
19. Meng Wang, G. Audi, F. G. Kondev, W. J. Huang, S. Naimi, and Xing Xu, Chin. Phys. C **41**, 030003 (2017).
20. W. D. Myers and W. J. Swiatecki, Nucl. Phys. A **601**, 141 (1996).
21. R. N. Sagaidak, IL NUOVO CIMENTO **42 C**, 69(2019).
22. K.H. Schmidt, Eur. Phys. J. A **8**, 141 (2000).
23. H. Haba *et al*., Phys. Rev. C **83**, 034602 (2011).
24. F. P. Heβberger, S. Antalic, F. Giacoppo, B. Andel, D. Ackermann, M. Block, S. Heinz, J. Khuyagbaatar, I. Kojouharov, and M. Venhart, Eur. Phys. J. A **58**, 11 (2022).
25.A. N. Kuzmina, G. G. Adamian, and N. V. Antonenko, Phys. Rev. C **85**, 027308 (2012); G. G. Adamian, private communication.
26. G. Audi, F. G. Kondev, Meng Wang, W. J. Huang, and S. Naimi, Chin. Phys**. 41**, 030001 (2017).
27.A. Såmark-Roth *et al*., Phys. Rev. Lett. **126**, 032503 (2021).
28. V. I. Zagrebaev, A.V. Karpov, Y. Aritomo, M. Naumenko, W. Greiner, Phys. Part. Nucl., **38**, 469 (2007).
29. J. Maruhn and W. Greiner, Z. Phys. A **251**, 431(1972).
30. P. Jachimowicz, M. Kowal, and J. Skalski, At. Data Nucl. Data Tables **138**, 101393(2021).
31. D. Inglis, Phys. Rev. **96**, 1059(1954).
32. S. N. Kuklin, T. M. Shneidman, G. G. Adamian, and N. V. Antonenko, Eur. Phys. J. A **48**, 112(2012).

33. F. P Heβberger, EPJ Web of Conferences **131**, 02005 (2016).
34. Yu. Ts. Oganessian *et al*., Phys. Rev. C **87**, 014302 (2013).
35. A. G. Popeko, Nucl. Instrum. Methods Phys. Res. B **376**, 144 (2016).
36. D. I. Solovyev and N. D. Kovrizhnykh, Journal of Instrumentation **17**, P07033 (2022).